A MEMS-boosted Over-the-Air RF Energy Harvester for IoT Receivers

Luca Colombo*, Giuseppe Michetti*, Gabriel Giribaldi*, Nicolas Casilli*, Ankit Mittal*, Guodong Zhang†, Patrick Cabrol†, Aatmesh Shrivastava*, Cristian Cassella*, and Matteo Rinaldi*
*SMART Center, Northeastern University, Boston MA, USA
†InterDigital Inc., New York NY, USA

***Abstract*—In this work, a novel over-the-air (OTA) radio frequency (RF) energy harvester (EH) architecture implementing a microelectromechanical system (MEMS) as matching network is presented. The system operates at a frequency of 820 MHz and is composed of a sub-50 Ω single-meandered antenna on printed circuit board, a MEMS film bulk acoustic resonator (FBAR), and a Schkotty diode half-bridge full wave rectifier followed by a sample-and-hold circuit.**

Experimental results demonstrate that the inclusion of the FBAR leads to an improvement of the energy harvester's efficiency, resulting in a 8-fold increase of the harvested power compared to a system without the MEMS resonator. This first demonstration of an increased efficiency over-the-air energy harvester implementing MEMS resonator representS an encouraging and viable solution for ultra-low or zero-power electronic devices for Internet of Things applications, including distributed and remote sensor networks.

***Index Terms*—IoT, Energy Harvester, MEMS, Rectifier, Antenna**

I. Introduction

THE development of Internet of Things (IoT) technologies has been an area of significant growth and innovation in recent years [1] [2]. In the IoT space, event-driven remote sensor networks are an appealing solution to collect data forming a decentralized, low-power, and low-cost system. These sensors are specifically designed to be left in place for long periods of time without the need for regular maintenance or battery replacement, operating in stand-by mode with nW power absorption, therefore consuming higher power only when triggered by a physical or radio frequency (RF) trigger [3].

To increase the battery lifetime of these nodes, one of the proposed solutions is the use of energy harvesters (EHs) [4], which are devices that convert ambient energy from sources such as light, vibration, or temperature differences, into the electrical energy that powers the sensor. Harvesting energy to drive the circuit consequently reduces the need for battery replacement, increasing the sensor's lifetime. This technology is particularly useful in remote or inaccessible locations where regular maintenance is difficult or impossible [5].

While still embodying a promising technological solution for the synthesis of RF ultra low power (ULP) or zero energy (ZE) receivers (Rx) [6], EHs suffer from limited conversion efficiency due to the minimum RF voltages required by the non-linear components to trigger RF-to-DC rectification (typically in the mV range) [7].

In this paper, we present a novel over-the-air (OTA) EH architecture that utilizes microelectromechanical systems (MEMS) as matching networks (MNs) to improve EH performance, resulting in increased lifetime of ULP Rx for IoT applications. To the knowledge of the authors, this represents the first demonstration of MEMS-boosted energy harvester for IoT applications.

High-performance MEMS resonators exploiting different materials [8] [9] [10] and resonant modes [11] [12] [13] have been successfully implemented as MNs to passively amplify RF signals in ULP architectures. In this work, a custom-made aluminum nitride (AlN) thin-film bulk acoustic resonator (FBAR) is deployed as a high-quality factor MN. In the first section of this work, the EH architecture is introduced, together with design and optimization techniques for its constituting elements. In the second section, the OTA measurement setup and results are reported. Lastly, in the conclusions section, we discuss how to further improve the circuit architecture and its potential to greatly improve the efficiency of IoT distributed networks.

II. Energy Harvester Architecture

A high-level schematic of an envisioned RF zero energy receiver for a distributed IoT sensing network is reported in Fig. 1. The system is composed by a multi-port antenna feeding an information receiver (IRx) branch, an energy harvester (EH) branch, and a rechargeable battery. Despite containing active components in the IRx , the proposed ZE Rx requires no external energy, relying solely on the power supplied by the EH.

The OTA EH proposed in this work represents a building block of the envisioned ZE Rx and is composed of a planar

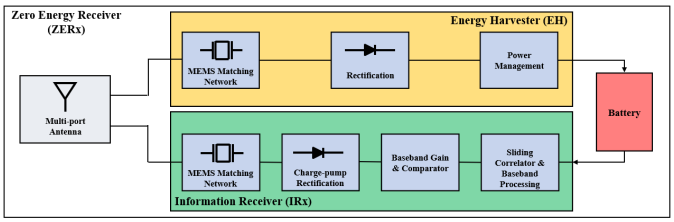

Fig. 1. Proposed zero energy receiver (ZE Rx) architecture, composed by a multi-port antenna, a energy harvester branch, an information receiver branch, and a rechargeable battery.

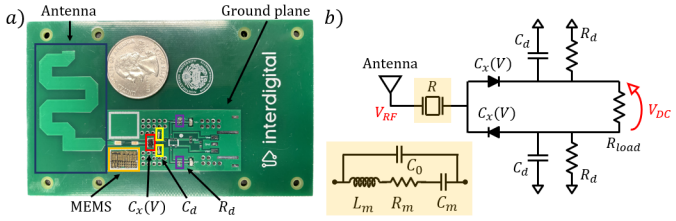

Fig. 2. a) Manufactured over-the-air energy harvester demo with a quarter US dollar for size comparison. The system is composed by a low-impedance antenna manufactured on a printed circuit board (PCB), a MEMS-based matching network, two antiparallel Schottky diodes $C_x(V)$ (Model: Onsemi®SBX201C), two capacitors (C_d = 120 pF), and two resistances (R_d = 5 kΩ). The MEMS-based matching network is connected to the circuit board via wire-bonding; and b) Circuit diagram of the system. The antiparallel diode acts as a rectifier to convert RF power to DC, while C_d and R_d are in place as a sample-and-hold circuit. R_{load} represents the load resistance and, for the case under investigation, is located off-board.

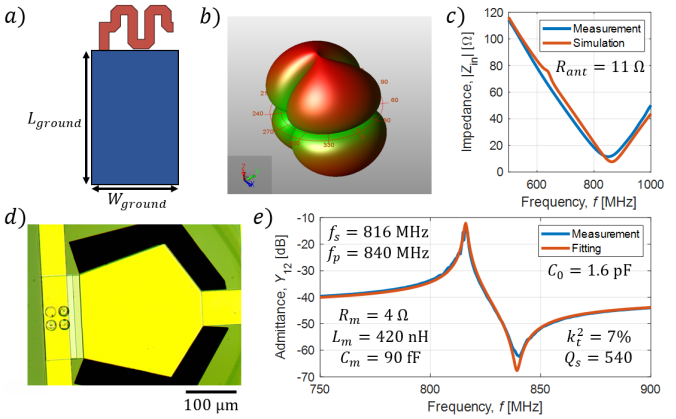

Fig. 3. a) Schematic of the implemented single-dipole meandered antenna. The metal plane is sized to provide a strong ground for the antenna and mimic the presence of a second dipole while breaking the system's symmetry; b) ADS Momentum® simulated radiation pattern; c) Comparison between the simulated and the measured antenna impedance response (Z). The antenna operates around 800 MHz and its minimum impedance is 11 Ω; d) Microscope image of an in-house fabricated aluminum nitride MEMS film bulk acoustic resonator (FBAR); and e) Measured admittance response of the FBAR implemented for the energy harvester demo.

antenna, a MEMS-based matching network, and a power management unit. For the sake of prototyping, the antenna is optimized for a single frequency and the power management unit is substituted by a simple resistive load to evaluate the conversion efficiency of the OTA EH. Pictures of the manufactured prototype and of its equivalent circuit are reported in Fig. 2a and b, respectively. The system implements a self-resonant antenna operating around 820 MHz realized on PCB FR-4 substrate, an in-house fabricated MEMS thin-Film Bulk Acoustic Resonator (FBAR) as matching network, two antiparallel Schkotty diodes ($C_x(V)$) arranged in a half-bridge full-wave rectifier, and an RC sample-and-hold circuit constituted by capacitance (C_d) and resistance (R_d) for each of the rectifier's output branches. The PCB board presents two output pins to interface the circuit to a variable load (R_{load}) for DC voltage and rectified power measurement. A meandered dipole design is chosen for the RF antenna [14], to minimize antenna aspect-ratio and offer low radiation resistance. The dimensions of the meander (length and turns) are set to ensure a resonance ∼820 MHz and sub-50 Ω impedance ($|Z_{in}|$) at the desired frequency of operation. The ground plane geometry (L_{ground} and W_{ground}, Fig. 3a) is appropriately designed to allow the adoption of a single-meandered antenna in place of a double-meandered configuration. By breaking the antenna's symmetry, is possible to interface the meandered antenna to a single-ended circuit while reducing any return loss and providing a solid ground for the other EH components.

Near omni-directional radiation, as expected for dipole antenna, is simulated via ADS Momentum ®(Fig. 3b). Simulated $|Z_{in}|$ is verified experimentally after proper de-embedding on an identical manufactured board provided with an SMA access port (Fig. 3c). The resonator implemented for the prototype is an in-house fabricated AlN FBAR (Fig. 3d) operating at 817 MHz [15] [16] [17], with a quality factor (Q_s) of 500 and a electromechanical coupling (k_t^2) of 7% (Fig. 3e), interfaced to the circuit via wire-bonding.

During the OTA EH operation, the RF radiation is transduced by the antenna and converted into an electrical signal. The MEMS matching network resonates out the capacitance of the diode at the desired frequency of operation, building up a large voltage gain across C_x. Thanks to its non-linear behavior, the half-bridge full-wave rectifier converts the RF signal to DC. The presence of the MEMS allows larger voltages across the diode, which ultimately increases the system's efficiency. Ultimately, the sample and hold capacitor (C_d) is used to maintain a constant DC output voltage from the rectifier, while R_d provides a stable reference bias to the diode.

III. Measurements and Results

The experimental setup for the OTA EH demo is reported in Fig. 4. The transmitter (Tx) consists of an RF generator, an RF amplifier, a power source to power the amplifier, and a high-gain (+4 dBi) broad-band directional antenna (Model: Aaronia HyperLOG 4025). The amplifier is used to add 30 dBi gain to the continuous wave (CW) signal provided by the RF generator to compensate for the estimated path loss of the experimental setup. The OTA EH is placed 0.5 m from the antenna on a plastic holder and is connected to a resistance decade box (Z-box) via mini hook cables. A digital multimeter is connected in parallel to the Z-box to monitor both the load (R_{load}) and the rectified voltage (V_{DC}). For the case under investigation, the load is set to 10 kΩ.

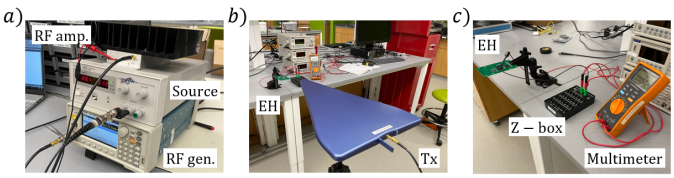

Fig. 4. Experimental setup, consisting in: a) RF generator and amplifier; b) transmitting directional, high-gain, broad-band antenna mounted on a tripod; and c) EH demo, located 0.5 m from the antenna. A manually tunable Z box is used as a load resistance (R_{load}) to calculate the rectified power. The voltage absorbed by Z_{load} is measured with a digital multimeter.

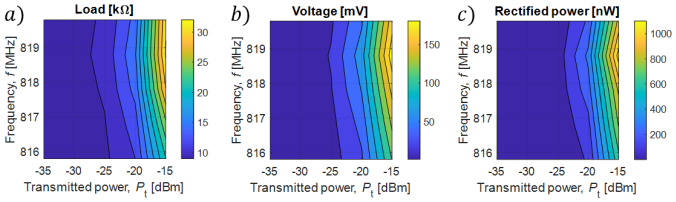

Fig. 5. Measured a) load resistance; b) voltage (V_{load}); and c) power absorbed by Z_{load} when implementing the MEMS FBAR as matching network (MN). The circuit implementing the MEMS showcases a 8x improvement in harvested power.

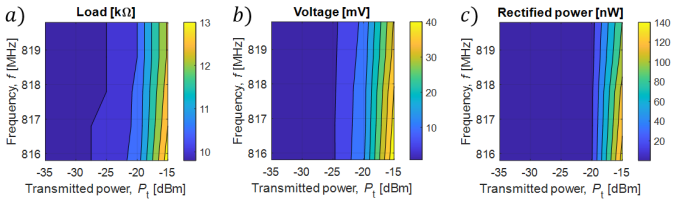

Fig. 6. Measured a) load resistance; b) voltage (V_{load}); and c) power absorbed by Z_{load} without the MEMS.

Fig. 6 and Fig. 5 report the measured load, voltage, and harvested power for the same OTA EH implementing the FBAR MEMS matching network and without the matching network, respectively. The frequency is swept around the series resonance of the MEMS, to take into account for frequency pulling [18], while the power is varied between -35 and -15 dBm. As clearly highlighted by the experimental results, the presence of the matching network introduces a frequency-dependent voltage boost, which directly translates to an 8-fold increase in the harvested power.

IV. Conclusions

In this work, we demonstrated for the first time the effectiveness of using MEMS resonators as matching networks to boost RF-to-DC conversion efficiency in over-the-air energy harvesters for IoT applications. Experimental results showed a 8-fold improvement in the rectified power output at 800 MHz when implementing an aluminum nitride FBAR as a matching element. Despite the limited efficiency attained, these results have important implications for the development of ultra low power or zero energy receivers, and further research is needed to explore the full potential of MEMS technology for these applications. Implementing higher figure of merit (FOM) [10], low threshold diodes, and matching the self-resonant antenna's impedance to the matched load could significantly improve the EHs rectification performance, making them more efficient and cost-effective. Overall, these results indicate that MEMS resonators are a promising solution for improving voltage rectification in energy harvester, and to potentially enable the development and deployment of sustainable, distributed sensing networks.

References

[1] I. F. Akyildiz, T. Melodia, and K. R. Chowdhury, "A survey on wireless multimedia sensor networks," *Computer Networks*, vol. 51, no. 4, pp. 921–960, 2007.

[2] L. Atzori, A. Iera, and G. Morabito, "The Internet of Things: A survey," *Computer Networks*, vol. 54, no. 15, pp. 2787–2805, 2010.

[3] P. Bassirian, J. Moody, and S. M. Bowers, "Event-driven wakeup receivers: Applications and design challenges," in *2017 IEEE 60th International Midwest Symposium on Circuits and Systems (MWSCAS)*, pp. 1324–1327, 2017.

[4] N. Mohd Yunus, J. Sampe, J. Yunas, and A. Pawi, "MEMS Based RF Energy Harvester for Battery-Less Remote Control: A Review," *American Journal of Applied Sciences*, vol. 14, 2017.

[5] R. H. Olsson, R. B. Bogoslovov, and C. Gordon, "Event driven persistent sensing: Overcoming the energy and lifetime limitations in unattended wireless sensors," in *2016 IEEE SENSORS*, pp. 1–3, 2016.

[6] T. Haque, H. Elkotby, P. Cabrol, R. Pragada, and D. Castor, "A Supplemental Zero-Energy Downlink Air-Interface Enabling 40-Year Battery Life in IoT Devices," in *GLOBECOM 2020 - 2020 IEEE Global Communications Conference*, pp. 1–6, 2020.

[7] S.-Y. Lee, Z.-X. Liao, and C.-H. Lee, "Energy-Harvesting Circuits With a High-Efficiency Rectifier and a Low Temperature Coefficient Bandgap Voltage Reference," *IEEE Transactions on Very Large Scale Integration (VLSI) Systems*, vol. 27, no. 8, pp. 1760–1767, 2019.

[8] M. E. Galanko Klemash, S. S. Bedair, D. A. Diamond, R. Q. Rudy, V. F.-G. Tseng, J. S. Pulskamp, and I. Kierzewski, "1-Port Piezoelectric Resonators With $>$ 100 V/V Gain," *Journal of Microelectromechanical Systems*, vol. 29, no. 5, pp. 874–880, 2020.

[9] S. S. Bedair, J. S. Pulskamp, R. Rudy, R. Polcawich, R. Cable, and L. Griffin, "Boosting MEMS Piezoelectric Transformer Figures of Merit via Architecture Optimization," *IEEE Electron Device Letters*, vol. 39, no. 3, pp. 428–431, 2018.

[10] L. Colombo, M. E. G. Klemash, T. M. Kiebala, S. S. Bedair, G. Piazza, and M. Rinaldi, "VHF and UHF Lithium Niobate MEMS Resonators Exceeding 30 dB of Passive Gain," *IEEE Electron Device Letters*, vol. 42, no. 12, pp. 1853–1856, 2021.

[11] P. Bassirian, J. Moody, A. Gao, T. Manzaneque, B. H. Calhoun, N. S. Barker, S. Gong, and S. M. Bowers, "A passive 461 MHz AlN-CMOS RF front-end for event-driven wakeup receivers," in *2017 IEEE SENSORS*, pp. 1–3, 2017.

[12] C. Cassella, G. Chen, Z. Qian, G. Hummel, and M. Rinaldi, "920 MHZ ALUMINUM NITRIDE CROSS-SECTIONAL LAMÉ MODE PIEZOELECTRIC MEMS TRANSFORMER WITH HIGH OPEN-CIRCUIT VOLTAGE GAIN IN EXCESS OF 39," pp. 412–415, 05 2016.

[13] Y.-H. Song and S. Gong, "Arraying SH0 Lithium Niobate laterally vibrating resonators for mitigation of higher order spurious modes," pp. 111–114, 01 2016.

[14] T. Warnagiris and T. Minardo, "Performance of a meandered line as an electrically small transmitting antenna," *IEEE Transactions on Antennas and Propagation*, vol. 46, no. 12, pp. 1797–1801, 1998.

[15] G. Michetti, G. Giribaldi, M. Pirro, A. Mittal, T. Haque, P. Cabrol, R. Pragada, H. Elkotby, L. Colombo, A. Shrivastava, and M. Rinaldi, "Hybridly Integrated MEMS-IC RF Front-End for IoT with Embedded Filtering and Passive Voltage Amplification," in *2021 IEEE Sensors*, pp. 1–4, 2021.

[16] R. Ruby, P. Bradley, Y. Oshmyansky, A. Chien, and J. Larson, "Thin film bulk wave acoustic resonators (fbar) for wireless applications," in *2001 IEEE Ultrasonics Symposium. Proceedings. An International Symposium (Cat. No.01CH37263)*, vol. 1, pp. 813–821 vol.1, 2001.

[17] J. Segovia-Fernandez, J. M. Tsai, J. Do, H. Rashtian, X. Jiang, X. Liu, Y. Liu, and D. A. Horsley, "Monolithic aln mems-cmos resonant transformer for wake-up receivers," in *2017 IEEE International Ultrasonics Symposium (IUS)*, pp. 1–4, 2017.

[18] L. Colombo, A. Kochhar, G. Vidal-Álvarez, and G. Piazza, "High-Figure-of-Merit X-Cut Lithium Niobate MEMS Resonators Operating Around 50 MHz for Large Passive Voltage Amplification in Radio Frequency Applications," *IEEE Transactions on Ultrasonics, Ferroelectrics, and Frequency Control*, vol. 67, no. 7, pp. 1392–1402, 2020.